Improved bounds on elastic and transport properties of fiber-reinforced composites: Effect of polydispersivity in fiber radius

C. A. Miller
Department of Mechanical and Aerospace Engineering, North Carolina State University, Raleigh, North Carolina 27695-7910

S. Torquato[a)]
Department of Mechanical and Aerospace Engineering and Department of Chemical Engineering, North Carolina State University, Raleigh, North Carolina 27695-7910

(Received 1 August 1990; accepted for publication 2 November 1990)

Improved rigorous bounds on the effective elastic and transport properties of a transversely isotropic fiber-reinforced material composed of oriented, infinitely long, multisized circular cylinders distributed throughout a matrix are computed. Specifically, we evaluate such bounds on the effective axial shear modulus (which includes, by mathematical analogy, the transverse conductivity), effective transverse bulk modulus, and the effective transverse shear modulus. These are generally demonstrated to provide significant improvement over the Hill–Hashin bounds which incorporate only volume-fraction information. Although the upper bounds diverge from the lower bounds when the cylinders are much stiffer than the matrix, the improved lower bounds still yield relatively accurate estimates of the effective properties. Generally, increasing the degree of polydispersivity in cylinder size increases the effective transverse conductivity (or axial shear modulus) and effective transverse bulk modulus, and decreases (slightly) the effective transverse shear modulus for cases in which the fibers are more conducting or stiffer than the matrix.

I. INTRODUCTION

Rigorous upper and lower bounds on the effective properties of composite materials are useful because[1,2] (i) they enable one to test the merits of a theory or computer experiment; (ii) as successively more microstructural information is incorporated, the bounds become progressively narrower; and (iii) one of the bounds can typically provide a relatively accurate estimate of the property, even when the reciprocal bound diverges from it.

For transversely isotropic two-phase composites, Hill[3] and Hashin[4,5] obtained the best possible bounds on the effective axial shear modulus μ_e (or, equivalently, effective transverse conductivity σ_e), effective transverse bulk modulus k_e, and effective transverse shear modulus G_e, given the phase properties and volume fractions ϕ_i. Although bounds which improve upon these second-order bounds have been available for some time now,[6–8] their application has been, until recently, very slow because of the difficulty involved in ascertaining the statistical correlation functions involved.

In the last few years, improved bounds on the aforementioned effective properties[6–8] have been evaluated for nontrivial model microstructures consisting of random arrays of infinitely long, oriented cylinders in a matrix[9–14] by utilizing the analytical representations of the correlation functions derived by Torquato and Stell.[15,16] In particular, Torquato and Beasley[9,10] and Joslin and Stell[11] independently computed improved bounds due to Silnutzer[6] and to Milton[7,8] for *identical* overlapping (i.e., randomly centered) cylinders. Joslin and Stell[12] evaluated the same bounds for *polydispersed* overlapping cylinders and showed that the bounds were insensitive to polydispersivity for this microgeometry. Torquato and Lado,[13,14] and Smith and Torquato[17] calculated these improved bounds for *identical* nonoverlapping or impenetrable cylinders. This is a useful model of unidirectional fiber composites. For impenetrable cylinders, the effect of polydispersivity in cylinder size on these effective properties has heretofore not been rigorously studied. Unlike the case of overlapping cylinders, the effect of polydispersivity in cylinder size for impenetrable cylinders is generally expected to be significant.

The purpose of this paper is to compute improved bounds on μ_e (or σ_e), k_e, and G_e for composites consisting of random distributions of infinitely long, oriented, impenetrable cylinders with a polydispersivity in size. Such an investigation will enable us to study the effect of polydispersivity on the elastic and transport properties of such unidirectional composites.

II. IMPROVED BOUNDS ON THE EFFECTIVE ELASTIC MODULI

For a two-phase, transversely isotropic fiber-reinforced material, Hill[3] and Hashin[4,5] derived the best possible bounds on μ_e, k_e, and G_e given only the phase volume fractions ϕ_1 and ϕ_2, bulk moduli K_1 and K_2, and shear moduli

[a)] Author to whom all correspondence should be addressed.

 0021-8979/91/041948-08$03.00

G_1 and G_2. These are referred to as second-order bounds since they are exact through second order in the difference in phase properties. Silnutzer[6] derived improved third-order bounds on μ_e, k_e, and G_e that depend upon two integrals over certain three-point correlation functions. The Silnutzer bounds were simplified by Milton[7] and are, respectively, given for the axial shear modulus, transverse bulk modulus, and transverse shear modulus by

$$\mu_L^{(3)} \leqslant \mu_e \leqslant \mu_U^{(3)}, \tag{1}$$

where

$$\mu_U^{(3)} = \left(\langle G \rangle - \frac{\phi_1 \phi_2 (G_2 - G_1)^2}{\langle \tilde{G} \rangle + \langle G \rangle_\zeta} \right), \tag{2}$$

$$\mu_L^{(3)} = \left(\langle 1/G \rangle - \frac{\phi_1 \phi_2 (1/G_2 - 1/G_1)^2}{\langle 1/\tilde{G} \rangle + \langle 1/G \rangle_\zeta} \right)^{-1}, \tag{3}$$

$$k_L^{(3)} \leqslant k_e \leqslant k_U^{(3)}, \tag{4}$$

where

$$k_U^{(3)} = \left(\langle k \rangle - \frac{\phi_1 \phi_2 (k_2 - k_1)^2}{\langle \tilde{k} \rangle + \langle G \rangle_\zeta} \right), \tag{5}$$

$$k_L^{(3)} = \left(\langle 1/k \rangle - \frac{\phi_1 \phi_2 (1/k_2 - 1/k_1)^2}{\langle 1/\tilde{k} \rangle + \langle 1/G \rangle_\zeta} \right)^{-1}, \tag{6}$$

and

$$G_L^{(3)} \leqslant G_e \leqslant G_U^{(3)}, \tag{7}$$

where

$$G_U^{(3)} = \left(\langle G \rangle - \frac{\phi_1 \phi_2 (G_2 - G_1)^2}{\langle \tilde{G} \rangle + \Theta} \right), \tag{8}$$

$$G_L^{(3)} = \left(\langle 1/G \rangle - \frac{\phi_1 \phi_2 (1/G_2 - 1/G_1)^2}{\langle 1/\tilde{G} \rangle + \Xi} \right)^{-1}, \tag{9}$$

$$\Theta = [2\langle k \rangle_\zeta \langle G \rangle^2 + \langle k \rangle^2 \langle G \rangle_\eta] / \langle k + 2G \rangle^2, \tag{10}$$

$$\Xi = 2\langle 1/k \rangle_\zeta + \langle 1/G \rangle_\eta. \tag{11}$$

Here we define $\langle b \rangle = b_1\phi_1 + b_2\phi_2$, $\langle \tilde{b} \rangle = b_1\phi_2 + b_2\phi_1$, $\langle b \rangle_\zeta = b_1\zeta_1 + b_2\zeta_2$, and $\langle b \rangle_\eta = b_1\eta_1 + b_2\eta_2$. The quantity k_i is the transverse bulk modulus of phase i for transverse compression without axial extension and may be expressed in terms of the isotropic phase moduli as $k_i = K_i + G_i/3$ $(i = 1,2)$. The parameters $\zeta_2 = 1 - \zeta_1$ and $\eta_2 = 1 - \eta_1$ are integrals over the two- and three-point probability functions $S_2(r)$ and $S_3(r,s,t)$, and are defined by

$$\zeta_2 = \frac{4}{\pi \phi_1 \phi_2} \int_0^\infty \frac{dr}{r} \int_0^\infty \frac{ds}{s} \int_0^\pi d\theta \times \left(S_3(r,s,t) - \frac{S_2(r) S_2(s)}{\phi_2} \right) \cos 2\theta, \tag{12}$$

and

$$\eta_2 = \frac{16}{\pi \phi_1 \phi_2} \int_0^\infty \frac{dr}{r} \int_0^\infty \frac{ds}{s} \int_0^\pi d\theta \times \left(S_3(r,s,t) - \frac{S_2(r) S_2(s)}{\phi_2} \right) \cos 4\theta. \tag{13}$$

The quantities $S_2(r)$ and $S_3(r,s,t)$ are, respectively, the probabilities of finding in phase 2 the end points of a line segment of length r and the vertices of a triangle with sides of length r, s, and t; θ is the included angle opposite the side of length t.

For $\zeta_2 = \eta_2 = 0$, the above third-order bounds coincide and equal the corresponding second-order Hill–Hashin lower bounds for cases in which phase 2 is stiffer than phase 1. For $\zeta_2 = \eta_2 = 1$, the bounds coincide and equal the corresponding Hill–Hashin upper bounds for instances in which phase 2 is stiffer than phase 1. The third-order bounds always improve upon the second-order bounds of Hill and Hashin, since both ζ_i and η_i lie in the closed interval $[0,1]$. Hashin[5] showed that the problem of determining the effective axial shear modulus μ_e is mathematically equivalent to determining the effective transverse thermal or electrical conductivity σ_e. Hence, results for μ_e can be immediately translated into equivalent results for σ_e.

Milton[8] derived fourth-order bounds on the effective axial shear modulus μ_e or transverse conductivity σ_e of transversely isotropic fiber-reinforced materials that depend upon the phase properties ϕ_2, ζ_2, and an integral over the four-point probability function S_4. Milton showed that by utilizing a phase-change theorem, the integral involving S_4 can be expressed in terms of ϕ_2 and ζ_2 only. For the case $G_2 \geqslant G_1$, the fourth-order bounds are given by

$$\mu_L^{(4)} \leqslant \mu_e \leqslant \mu_U^{(4)}, \tag{14}$$

where

$$\mu_U^{(4)} = G_2 \left(\frac{(G_1 + G_2)(G_1 + \langle G \rangle) - \phi_2 \zeta_1 (G_2 - G_1)^2}{(G_1 + G_2)(G_2 + \langle \tilde{G} \rangle) - \phi_2 \zeta_1 (G_2 - G_1)^2} \right), \tag{15}$$

$$\mu_L^{(4)} = G_1 \left(\frac{(G_1 + G_2)(G_2 + \langle G \rangle) - \phi_1 \zeta_2 (G_2 - G_1)^2}{(G_1 + G_2)(G_1 + \langle \tilde{G} \rangle) - \phi_1 \zeta_2 (G_2 - G_1)^2} \right). \tag{16}$$

III. EVALUATION OF THE MICROSTRUCTURAL PARAMETERS FOR RANDOM ARRAYS OF POLYDISPERSED CYLINDERS

A. The three-point probability function S_3

To evaluate the integrals (12) and (13) for a polydispersed array of infinitely long, oriented, hard cylinders (disks in two dimensions), the three-point probability function S_3 must be determined. An exact infinite-series representation of the general n-point probability function S_n has been given by Torquato and Stell[15] for a two-phase system of d-dimensional identical spheres (phase 2) distributed throughout a matrix (phase 1). The S_n for random, polydispersed arrays of d-dimensional spheres can be determined by a straightforward generalization of the explicit expressions of the S_n derived by Torquato and Stell.[16] For statistically isotropic distributions of impenetrable disks, it has been shown[16] that the infinite series for S_n terminates with the nth term; for a system of impenetrable disks having a discrete distribution of M diameters a_i $(i = 1,...,M)$, in the case $n = 3$, it is given by

$$S_3(r_{12},r_{13},r_{23}) = S_3^{(1)}(r_{12},r_{13},r_{23}) + S_3^{(2)}(r_{12},r_{13},r_{23}) + S_3^{(3)}(r_{12},r_{13},r_{23}), \quad (17)$$

where

$$S_3^{(1)} = \sum_{i=1}^{M} \rho_i \int m_i(r_{14}) m_i(r_{24}) m_i(r_{34}) d\mathbf{r}_4, \quad (18)$$

$$S_3^{(2)} = \sum_{i=1}^{M} \sum_{j=1}^{M} \Big(\rho_i \rho_j \int\int m_i(r_{14}) m_i(r_{24}) m_j(r_{35}) \times g_{ij}(r_{45}) d\mathbf{r}_4\, d\mathbf{r}_5 + \rho_i \rho_j \int\int m_i(r_{14}) m_j(r_{25}) \times m_i(r_{34}) g_{ij}(r_{45}) d\mathbf{r}_4\, d\mathbf{r}_5 + \rho_i \rho_j \int\int m_j(r_{15}) \times m_i(r_{24}) m_i(r_{34}) g_{ij}(r_{45}) d\mathbf{r}_4\, d\mathbf{r}_5 \Big), \quad (19)$$

$$S_3^{(3)} = \sum_{i=1}^{M} \sum_{j=1}^{M} \sum_{k=1}^{M} \rho_i \rho_j \rho_k \int\int\int m_i(r_{14}) m_j(r_{25}) \times m_k(r_{36}) g_{ijk}(r_{45},r_{46},r_{56}) d\mathbf{r}_4\, d\mathbf{r}_5\, d\mathbf{r}_6, \quad (20)$$

with

$$m_i(r) = \begin{cases} 1, & r < a_i, \\ 0, & r > a_i. \end{cases} \quad (21)$$

Here ρ_i is the number density of disks (cylinders) of radius a_i, and therefore the disk area fraction (or cylinder volume fraction) ϕ_2 is given by the relation

$$\phi_2 = \sum_{i=1}^{M} \rho_i \pi a_i^2. \quad (22)$$

g_{ij} is the pair (radial) distribution function associated with particles of radii a_i and a_j, and g_{ijk} is the triplet distribution function for particles of radii a_i, a_j, and a_k, with $r_{ij} \equiv |\mathbf{r}_j - \mathbf{r}_i|$. The domain of integration in each of the above integrals in (18)–(20) is the infinite area of the macroscopic sample. Note that S_2 can be obtained from the expression for S_3 [Eq. (17)] by letting two of the three points coincide.

The three-dimensional analog of (17) through two-body terms (i.e., up to $S_3^{(2)}$) was utilized by Thovert *et al.*,[18] but was not stated explicitly by them. Torquato[2] has given a general discussion on correlation functions for polydispersed inclusions, and Lu and Torquato[19] have extended the formalism of Torquato[20] to obtain the so-called general n-point distribution function H_n for polydispersed suspensions, which contains result (17) as a special case.

B. The microstructural parameter ζ_2

It is clear from (17)–(20) and (12) that fivefold, sevenfold, and ninefold integrations must be carried out in order to evaluate the microstructural parameter ζ_2. Torquato and Lado[13] have greatly simplified these "cluster" integrals by expanding the angle-dependent terms in Chebyshev polynomials and using the orthogonality properties of these circular harmonics. We shall follow this procedure to compute ζ_2 for impenetrable disks with a polydispersivity in disk diameter.

We shall first exploit an important property of ζ_2 for distributions of d-dimensional spheres that only recently has fully come to light; namely, the low-volume-fraction expansion of ζ_2 provides a remarkably accurate approximation to the exact ζ_2 for a wide range of ϕ_2, with the term linear in ϕ_2 being the dominant one[21] (see also Ref. 2). This property, also true for the parameter η_2, has recently been employed by Thovert *et al.*,[18] Torquato,[20] and Torquato and Lado[14] in related problems. Such behavior has been verified by the computer simulation study of Miller and Torquato[21] for impenetrable spheres for virtually the entire volume-fraction range. It is also supported by the simulations of Smith and Torquato[17] for the nonequilibrium, random-sequential addition of hard disks. This implies that the calculation of ζ_2 in the superposition approximation by Torquato and Lado[13] (although accurate and approximately linear for $\phi_2 \leqslant 0.45$) overestimates ζ_2 for large ϕ_2 (i.e., $\phi_2 > 0.45$). The fact that ζ_2 is approximately linear for a wide range of ϕ_2 makes our task considerably easier since we only need to compute ζ_2 to leading order in ϕ_2, a result obtainable analytically. Thus our strategy is to evaluate (12) through first order in ϕ_2, implying that we need to substitute only the first two terms of (17) (i.e., up to two-body terms). After simplification, we find that

$$\zeta_2 = \frac{2\phi_2}{\pi\phi_1} b_2, \quad (23)$$

where

$$b_2 = \frac{\pi^3 \rho^2}{\phi_2^2} \int_0^\infty \int_0^\infty da\, db\, a^2 b^2 f(a) f(b) \times \int_{a+b}^\infty dr \frac{r a^2 g_2(r)}{(r^2 - b^2)^2}, \quad (24)$$

where $f(a)$ is the given (continuous) size distribution for particles of radius a, ρ is the total number density of disks, and g_2 is the pair (radial) distribution function for particles of radii a and b. Equation (24) is a polydispersed generalization of the monodispersed result first given by Torquato and Lado.[13] Torquato and Lado also gave the monodispersed three-body term.

Now $g_2(r)$ in (24) is generally a complicated function of density. However, since ζ_2 is to an excellent approximation linear for a wide range of ϕ_2, we need only employ the exact low-density limit ($\phi_2 \to 0$) of the radial distribution function,

$$g_2(r) = \begin{cases} 0, & r < a + b, \\ 1, & r > a + b, \end{cases} \quad (25)$$

in relation (24). As $\phi_2 \to 0$, combination of (23), (24), and (25) yields

$$\zeta_2 = \frac{\pi^2 \rho^2}{\phi_2} \int_0^\infty \int_0^\infty da\, db\, a^2 b^2 f(a) f(b) \Delta_\zeta\left(\frac{a}{b}\right) + O(\phi_2^2), \quad (26)$$

where

$$\Delta_\zeta\left(\frac{b}{a}\right) = 2 \int_{a+b}^\infty \frac{a^2 r\, dr}{(r^2 - b^2)^2} = \frac{1}{1 + 2a/b}. \quad (27)$$

Note that the term $\pi\rho a^2$ above will lead to a factor of ϕ_2 when integrated over a. When (26) is integrated over both a and b, a factor of ϕ_2^2 will arise, making the first term in (26)

of order ϕ_2 rather than of order ϕ_2^{-1} as it may appear. For discrete distributions of M different disk radii, $f(a)$ takes the form

$$f(a) = \sum_{i=1}^{M} \frac{\rho_i}{\rho} \delta(a - a_i) \tag{28}$$

where $\delta(a)$ is the Dirac δ function. For a monodispersed distribution of disks, $M = 1$ and $a = b$, (26) yields the $O(\phi_2)$ result of Torquato and Lado[13] for equisized disks:

$$\zeta_2 = \frac{\phi_2}{3} + O(\phi_2^2). \tag{29}$$

Torquato and Lado actually evaluated ζ_2 exactly through $O(\phi_2^2)$, but found that the linear term was by far the dominant one. The effects of polydispersivity are greatest for suspensions of fibers with widely separated radii, i.e., $b/a \to 0$. For a bidispersed suspension with widely separated fiber radii ($M = 2$) and a polydispersed suspension of M different ($M \to \infty$) and widely separated fiber radii, (26) yields, respectively,

$$\zeta_2 = \tfrac{5}{12}\phi_2 + O(\phi_2^2), \tag{30}$$

$$\zeta_2 = \frac{\phi_2}{2} + O(\phi_2^2). \tag{31}$$

Note that (31) is identical to that found in three dimensions by Thovert *et al.*[18] for a polydispersion of impenetrable spheres with widely separated sizes. Further, observe that (30) lies exactly midway between the monodispersed result (29) and (31).

Following Torquato and Lado,[14] we shall apply these low-density expansions for ζ_2 in the fiber volume-fraction range $0 \leqslant \phi_2 \leqslant 0.7$. The volume fraction $\phi_2 = 0.7$ corresponds to about 87% of the maximum random-close-packing value for monodispersions.[22] Thus, for polydispersions (which have a larger close-packing fraction), the linear results may be applied beyond $\phi_2 = 0.7$; however, this shall not be done here.

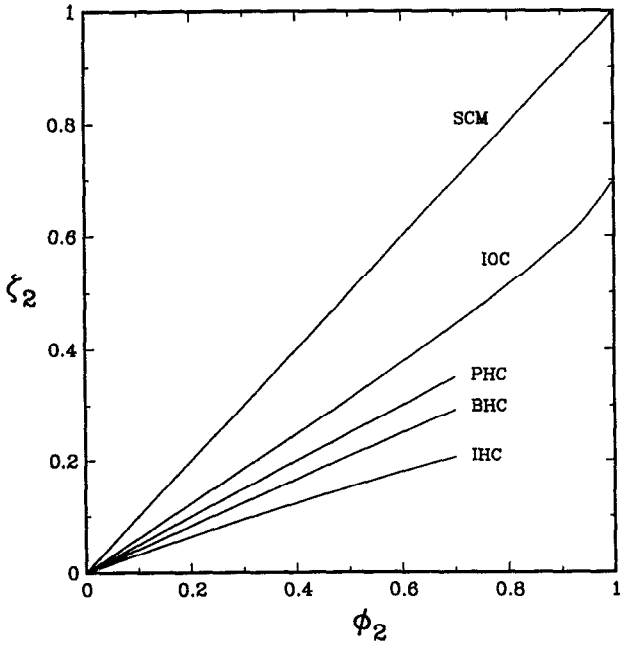

FIG. 1. Three-point parameter ζ_2, defined by Eq. (12), for three hard-cylinder microgeometries: identical hard cylinders (IHC) [Eq. (28)], bidispersed hard cylinders with widely spaced cylinder radii (BHC) [Eq. (30)], and polydispersed hard cylinders with widely spaced radii (PHC) [Eq. (31)]. Also included are ζ_2 for a symmetric-cell material (SCM) with cylindrical cells (see Refs. 7 and 23) and identical overlapping cylinders (IOC) (see Refs. 9 and 11).

In Fig. 1, we plot the parameter ζ_2 as given in Eq. (26) for the three hard-cylinder cases noted above in (29)–(31), i.e., the monodispersed case, the bidispersion with widely separated cylinder sizes, and the polydispersed case for widely separated cylinder sizes. For purposes of comparison, Fig. 1 also includes ζ_2 as calculated for symmetric-cell materials[23,24] and identical "fully penetrable" or "overlapping" cylinders[9,11] (i.e., spatially uncorrelated cylinders), each of which involves no approximation.

It is of interest to note that the effect of polydispersivity is to increase ζ_2 relative to equisized disks. One might initially expect the converse to be true since ζ_2 would then be approaching $\zeta_2 = 0$, the value corresponding to the well-known polydispersed composite-cylinder assemblage of Hashin[4,5] for the transverse conductivity (axial shear modulus) and transverse bulk modulus in the cases of more conducting or stiffer inner cylinders. These assemblages realize the second-order bounds. As noted by Torquato,[2] however, because the average separation distance between the inner cylinders in the composite-cylinder assemblage is larger than in the polydispersed, equilibrium hard-cylinder model examined here, the former construction inhibits clustering, and therefore ζ_2 for the present model should increase, rather than decrease, relative to the monodispersed result. This implies that the lower bounds on μ_e (or σ_e) and k_e, which turn out to yield good estimates of the effective properties in these instances,[2,13,14,25,26] will increase with increasing polydispersivity.

As seen in Fig. 1, the symmetric cell material result for $\zeta_2 = \phi_2$ appears to be an upper bound on ζ_2 for cylinders in all the geometries studied, be they overlapping or totally impenetrable equisized disks, or polydispersed disks; i.e.,

$$\zeta_2 \leqslant \phi_2. \tag{32}$$

This was first noted by Torquato and Lado,[13] but has yet to be rigorously proven. Torquato[2] has conjectured (32) to be true for a *class* of distributions of d-dimensional spheres. If shown to be rigorously true, then ζ_2 would be restricted to the closed interval $[0,\phi_2]$ for this class of geometries of cylinders rather than the wider interval $[0,1]$ which generally applies.

C. The microstructural parameter η_2

As was done in the previous section, η_2 is evaluated for polydispersed hard cylinders by first simplifying the cluster integrals which result after substituting (17)–(20) into (13). Again, using the circular-harmonics-expansion technique of Torquato and Lado,[13] the integral (13) can be significantly simplified (after considerable algebra). As in the case of ζ_2, the linear term of the low-volume-fraction expansion of η_2 should serve as a very good approximation to η_2 for a wide range of ϕ_2. Thus, we need only substitute the first two terms of (17) into (13) to obtain

$$\eta_2 = \frac{8\phi_2}{\pi\phi_1} c_2, \tag{33}$$

where

$$c_2 = \frac{\pi^2\rho^2}{\phi_2^2} \int_0^\infty \int_0^\infty da\, db\, a^2 b^2 f(a) f(b) \times \int_{a+b}^\infty dr\, r g_2(r) W(r), \tag{34}$$

$$W(r) = \frac{\pi a^2}{(r^2 - b^2)^2} \left(1 - \frac{3a^2}{(r^2 - b^2)} - \frac{9}{2} \frac{a^2 b^2}{(r^2 - b^2)^2} + \frac{9}{4} \frac{a^4}{(r^2 - b^2)^2} + 9 \frac{a^4 b^2}{(r^2 - b^2)^3} + \frac{15}{2} \frac{a^4 b^4}{(r^2 - b^2)^4} \right). \tag{35}$$

Relation (33) is the polydispersed generalization of the monodispersed result first obtained by Torquato and Lado;[14] the three-body term (not given here) was also derived by them for monodispersions.

Combination of (25), (33), (34), and (35) yields through first order in ϕ_2 that

$$\eta_2 = \frac{\pi^2\rho^2}{\phi_2} \int_0^\infty \int_0^\infty da\, db\, a^2 b^2 f(a) f(b) \Delta_\eta \left(\frac{a}{b} \right) + O(\phi_2^2), \tag{36}$$

where

$$\Delta_\eta \left(\frac{b}{a} \right) = 8 \int_{a+b}^\infty r W(r) dr = 8 \left(\frac{1}{2(1 + 2b/a)} - \frac{3}{4(1 + 2b/a)^2} - \frac{3}{4} \frac{(b/a)^2}{(1 + 2b/a)^3} + \frac{3}{8} \frac{1}{(1 + 2b/a)^3} + \frac{9}{8} \frac{(b/a)^2}{(1 + 2b/a)^4} + \frac{3}{4} \frac{(b/a)^4}{(1 + 2a/b)^5} \right). \tag{37}$$

Figure 2 compares the functions Δ_ζ and Δ_η as a function of the size ratio b/a.

Employing Eq. (28), one can then examine the behavior of η_2 for the three cases noted above for ζ_2, namely, the monodispersed result, and the widely spaced bidispersed and polydispersed suspensions. For these three cases, one finds, respectively,

$$\eta_2 = \tfrac{56}{81}\phi_2 + O(\phi_2^2), \tag{38}$$

$$\eta_2 = \tfrac{193}{324}\phi_2 + O(\phi_2^2), \tag{39}$$

$$\eta_2 = \tfrac{1}{2}\phi_2 + O(\phi_2^2). \tag{40}$$

As before, the result (38) recovers the result of Torquato and Lado[14] for a random distribution of equisized hard disks. For the aforementioned polydispersed microgeometries, η_2 (unlike ζ_2) decreases as the degree of polydispersivity increases, although the effect is much smaller than the increase observed for ζ_2. The polydispersed result (40) is identical to that found by Thovert *et al.*[18] for the analogous three-dimensional case, and again we note that the result (39) for a bidispersed suspension of fibers with widely separated fiber radii lies exactly midway between (38) and (40). In Fig. 3, we plot the preceding three results as well as the result for symmetric-cell materials[23,24] and random arrays of identical overlapping cylinders.[10,12]

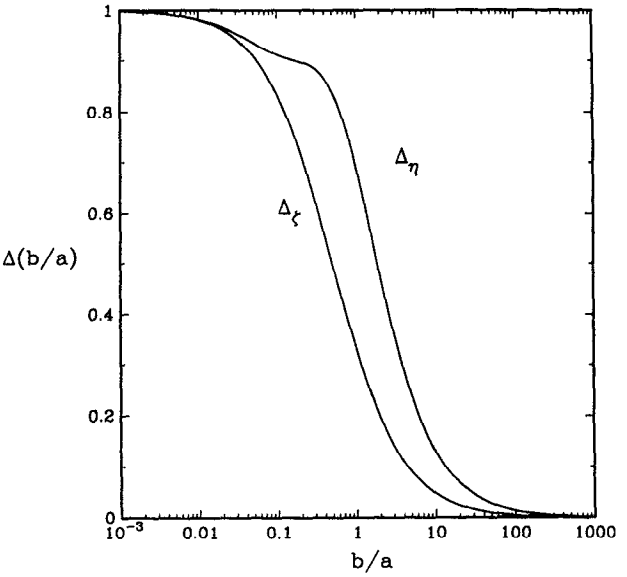

FIG. 2. The functions Δ_ζ (27) and Δ_η (37) as a function of the cylinder size ratio a/b.

We note that Torquato[2] has conjectured that for a *class* of distributions of d-dimensional spheres (e.g., symmetric-

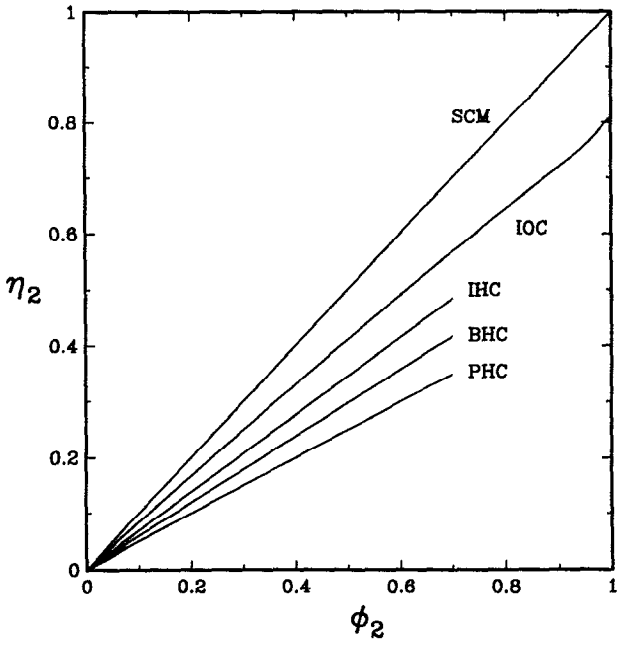

FIG. 3. Three-point parameter η_2, defined by Eq. (13), for three hard-cylinder microgeometries: identical hard cylinders (IHC) [Eq. (38)], bidispersed hard cylinders with widely spaced cylinder radii (BHC) [Eq. (39)], and polydispersed hard cylinders with widely spaced radii (PHC) [Eq. (40)]. Also included are ζ_2 for a symmetric-cell material (SCM) with cylindrical cells (see Refs. 7 and 23) and identical overlapping cylinders (IOC) (see Refs. 10 and 11).

cell materials with spherical or cylindrical cells, overlapping and impenetrable disks or spheres),

$$\eta_2 \geqslant \zeta_2. \tag{41}$$

He based this conjecture on observations for known results. He also noted that if (32) is true, then η_2 for d-dimensional spheres will lie in the more restricted closed interval $[\zeta_2, \phi_2]$ rather than the interval [0,1] which generally applies.

Note that the results above differ from the analogous results for hard spheres in two ways. First, for hard cylinders, increasing polydispersivity decreases η_2 from $\eta_2 = 56/81\phi_2$ for monodispersions [Eq. (38)] to $\eta_2 = 0.5\phi_2$ for polydispersions with widely spaced cylinder radii [Eq. (40)], while for hard spheres, η_2 increases from the monodispersed result $\eta_2 = 0.482\,74\phi_2$ to $\eta_2 = 0.5\phi_2$ for polydispersed hard spheres with widely spaced radii.[18] Second, the relative difference between the polydispersed and monodispersed values is considerably greater for hard cylinders than for hard spheres. This will lead to a significant difference in the behavior of the effective shear modulus for dispersions of hard spheres and the effective transverse shear modulus for suspensions of oriented hard cylinders.

A parameter η_2 which decreases as the degree of polydispersivity increases can have the effect of lowering the third-order bounds (7) on the transverse shear modulus G_e relative to the monodisperse result. [Note that unlike second-order bounds on μ_e (σ_e) and k_e, the second-order bounds on G_e are not achieved by composite-cylinder assemblages.[4]] In the case of perfectly rigid cylinders in an incompressible matrix, the results (38)–(40) and bounds (7) imply that G_e exactly, through third order in $(G_2 - G_1)$, must decrease as the polydispersivity increases for the hard-cylinder model.

IV. CALCULATION OF IMPROVED BOUNDS ON THE ELASTIC MODULI OF RANDOM ARRAYS OF POLYDISPERSED CYLINDERS

Here we employ the results (26) and (36) to compute the bounds presented in Eqs. (1)–(11) for suspensions of long, oriented, impenetrable cylinders with a polydispersivity in cylinder radius. We will examine cases in which the fiber stiffness (conductivity) is greater that that of the matrix in the range of fiber volume fractions $0 \leqslant \phi_2 \leqslant 0.7$. It should be noted that for the cases presented here, the lower bounds will provide a relatively accurate estimate of the effective property,[2,13,14,25,26] even when the bounds are not tight. This has recently been confirmed by exact determinations of the effective transverse conductivity (or effective axial shear modulus) for equilibrium distributions of hard cylinders obtained by Kim and Torquato.[27] This is due to the fact that the stiffer phase (fibers) can never form large connected clusters in the range of volume fractions considered here. Equilibrium distributions of cylinders do not form interparticle contacts until the random-close-packing volume fraction[22] ($\phi_2 \approx 0.81$) is reached.

In Fig. 4, we present third- and fourth-order bounds on the scaled effective transverse conductivity σ_e/σ_1 as calculated from Eqs. (1) and (14) as a function of the fiber volume fraction ϕ_2 for a composite with a conductivity ratio

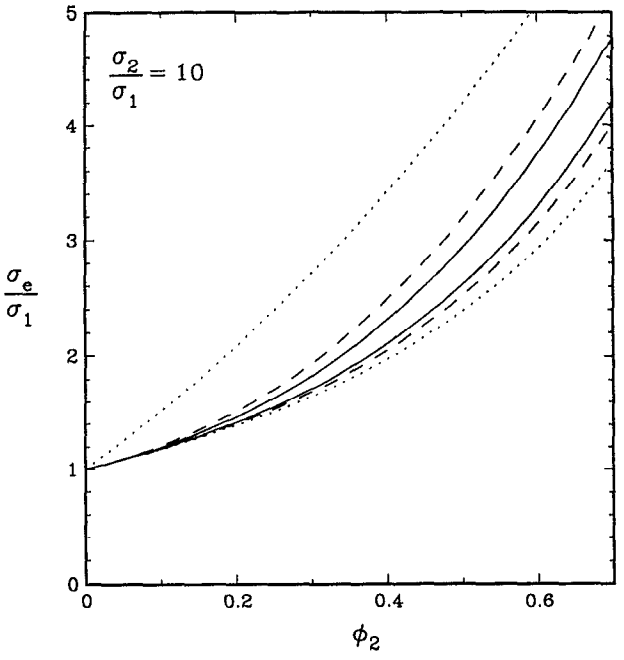

FIG. 4. Bounds on the scaled effective transverse conductivity σ_e/σ_1 vs the cylinder volume fraction ϕ_2 for an equilibrium distribution of polydispersed impenetrable cylinders with widely spaced cylinder radii [cf. Eq. (31)] at $\sigma_2/\sigma_1 = 10$; dotted curve, second-order bounds; (see Refs. 4 and 5) dashed curve, third-order bounds; (see Ref. 6) and solid curve, fourth-order bounds (see Ref. 8). These results can be immediately translated to equivalent results for the effective axial shear modulus (see Ref. 5).

$\sigma_2/\sigma_1 = 10$ for a distribution of polydispersed impenetrable cylinders with widely spaced radii, i.e., with ζ_2 given by (31). In these bounds we have replaced μ_e, G_1, and G_2 with σ_e, σ_1, and σ_2, respectively. Also included in the figure are the second-order upper and lower bounds derived by Hashin.[4,5] Observe that the third-order Silnutzer bounds are

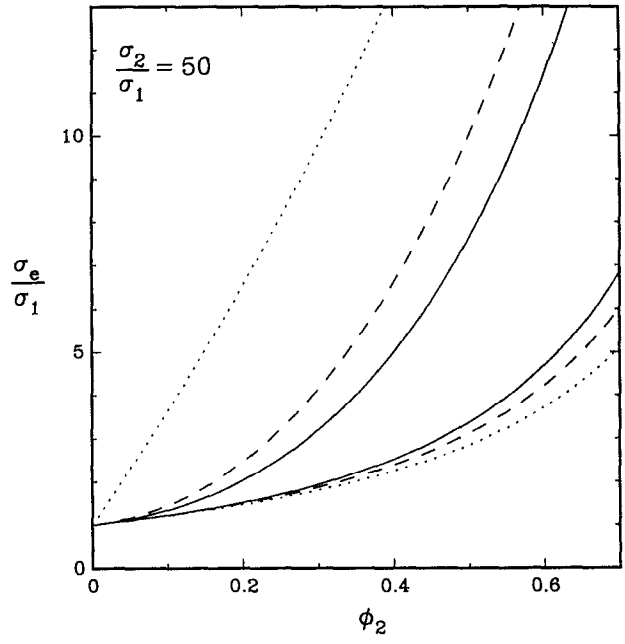

FIG. 5. As in Fig. 4, with $\sigma_2/\sigma_1 = 50$.

considerably more restrictive than the second-order Hashin bounds, and the fourth-order Milton bounds are a further improvement over the third-order bounds. The fourth-order lower bound provides an accurate estimate of the the effective transverse conductivity (or, equivalently, axial shear modulus) for the range of fiber volume fractions reported.

Figure 5 presents the same bounds for the case $\sigma_2/\sigma_1 = 50$. As expected, the bounds are wider than in the previous case, but as noted earlier, σ_e is still accurately estimated by the fourth-order lower bound.[14]

The case of superconducting fibers ($\sigma_2/\sigma_1 = \infty$) (or superrigid fibers in the case of the axial shear modulus) is presented in Fig. 6. Here, we present only the fourth-order lower bounds since the upper bounds diverge to infinity, but include the three cases (29)–(31) corresponding to monodispersed impenetrable cylinders, bidispersed impenetrable cylinders with widely spaced radii, and polydispersed impenetrable cylinders with widely spaced radii, respectively. The effect of polydispersivity is to increase the effective transverse conductivity or effective axial shear modulus.

In Fig. 7, we present the fourth-order bounds on the scaled effective axial shear modulus μ_e/G_1 [Eqs. (15) and (16)] as a function of the fiber volume fraction ϕ_2 for a glass-epoxy composite for which $G_2/G_1 = 22$ for three microgeometries of hard cylinders: monodispersed, bidispersed with widely spaced cylinder radii, and polydispersed with widely spaced radii [Eqs. (29)–(31)]. Also included are the corresponding second-order bounds.[4,5] The fourth-

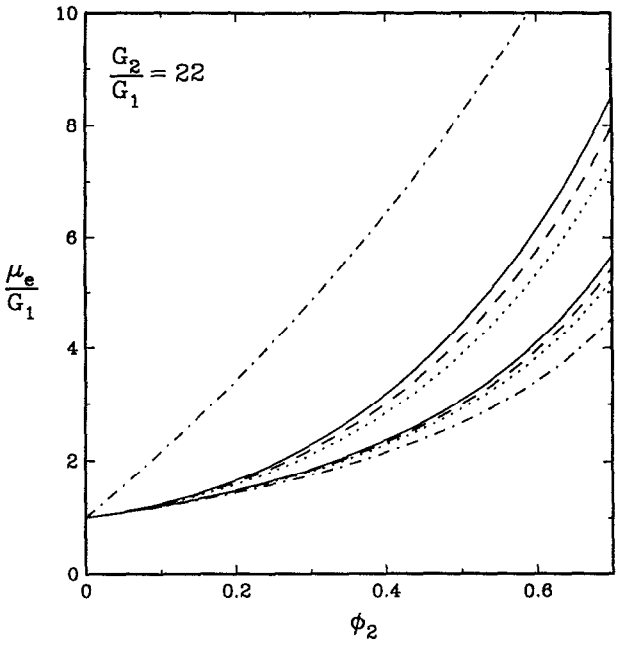

FIG. 7. Fourth-order bounds on the scaled axial shear modulus μ_e/G_1 for a glass-epoxy composite at $G_2/G_1 = 22$. Results for three microgeometries are given; dotted curve, monodispersed hard cylinders using (29); dashed curve, bidispersed hard cylinders with widely spaced cylinder radii using (30); solid curve, polydispersed hard cylinders with widely spaced cylinder radii using (31). Also included are the Hashin (see Refs. 4 and 5) two-point bounds (dot-dashed curve).

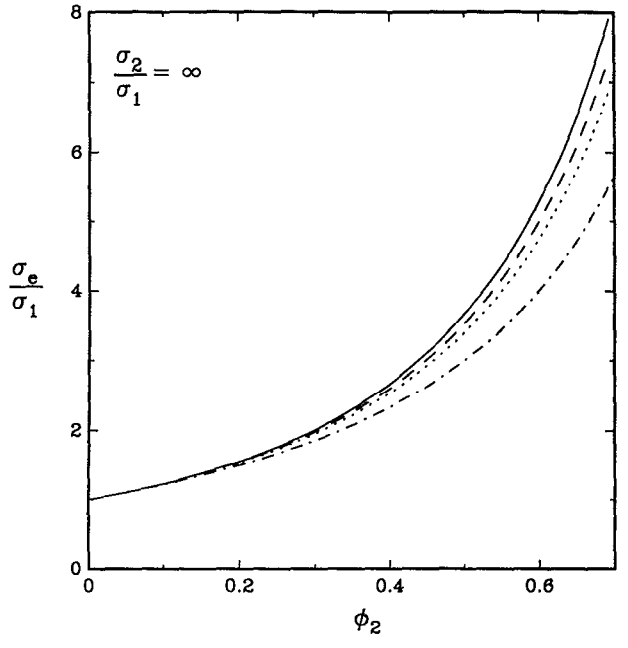

FIG. 6. Fourth-order lower bounds on the scaled effective transverse conductivity σ_e/σ_1 for three microgeometries of hard cylinders, at $\sigma_2/\sigma_1 = \infty$; dotted curve, monodispersed hard cylinders using (29); dashed curve, bidispersed hard cylinders with widely spaced cylinder radii using (30); solid curve, polydispersed hard cylinders with widely spaced cylinder radii using (31). Also included is the Hashin (see Refs. Ref. 4 and 5) two-point bound (dot-dashed curve). The corresponding upper bounds are not shown since they diverge to infinity in this limit.

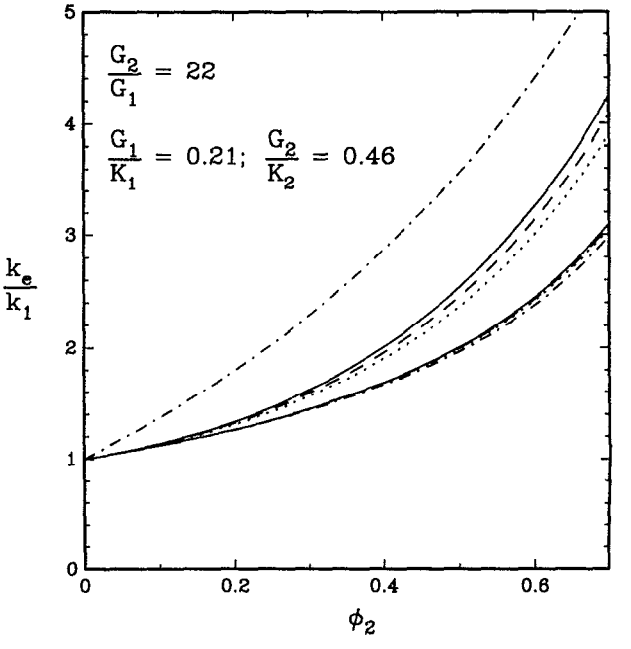

FIG. 8. Third-order bounds (see Ref. 6) on the scaled effective transverse bulk modulus k_e/k_1 vs the cylinder volume fraction ϕ_2 for glass-epoxy composites for which $G_2/G_1 = 22$, $G_1/K_1 = 0.21$, and $G_2/K_2 = 0.46$; dotted curve, monodispersed hard cylinders using (29); dashed curve, bidispersed hard cylinders with widely separated cylinder radii using (30); solid curve, polydispersed hard cylinders with widely spaced radii using (31). Included are the Hashin (see Refs. 4 and 5) two-point bounds (dot-dashed curve).

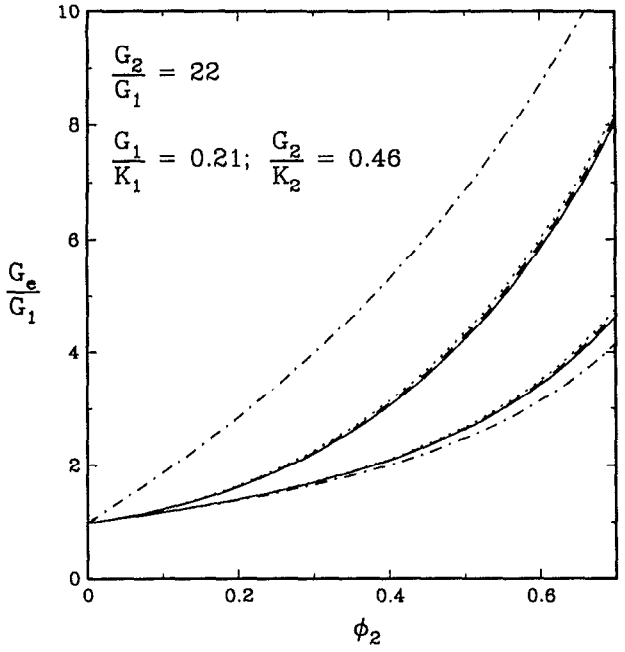

FIG. 9. Third-order bounds on the scaled effective transverse shear modulus G_e/G_1 for three microgeometries of hard cylinders for which $G_2/G_1 = 22$, $G_1/K_1 = 0.21$, and $G_2/K_2 = 0.46$; dotted curve, monodispersed hard cylinders using (38); dashed curve, bidispersed hard cylinders with widely separated cylinder radii using (39); solid curve, polydispersed hard cylinders with widely spaced radii using (40). Also included are the Hill–Hashin two-point bounds (see Refs. 4 and 5) (dot-dashed curve).

order bounds are considerably tighter than the second-order bounds and will yield good estimates of μ_e over a wide range of fiber volume fractions ϕ_2.

In Fig. 8, we compare the third-order Silnutzer bounds[6] on the scaled effective transverse bulk modulus k_e/k_1 for a glass-epoxy composite with $G_2/G_1 = 22$, $G_1/K_1 = 0.21$, and $G_2/K_2 = 0.46$ for three microgeometries: equisized hard cylinders, bidispersed hard cylinders with widely spaced radii, and polydispersed hard cylinders with widely spaced radii. The corresponding second-order bounds[3,4] are presented for comparison. Note that the effect of polydispersivity is to shift both upper and lower bounds upward.

Figure 9 presents third-order bounds[6] on G_e/G_1 with the same material properties as in Fig. 8 for equisized hard disks, bidispersed hard disks with widely spaced radii, and polydispersed hard disks with widely spaced radii. Included for comparison are the corresponding second-order bounds.[3,4] In the case of G_e, it can be seen that the effect of polydispersivity is to decrease the effective property.

As is clear from the results presented here, the effect of polydispersivity in cylinder size can either increase or decrease the effective property. For dispersions of impenetrable cylinders in general, an increase in polydispersivity will increase the effective transverse conductivity σ_e (or effective axial shear modulus μ_e) and the effective transverse bulk modulus k_e relative to the monodispersed case. In the case of the effective transverse shear modulus G_e, however, polydispersivity acts to *decrease* the effective property relative to the monodisperse case. This behavior is in contrast to that noted for three dimensions, i.e., dispersions of hard spheres. Thovert *et al.*[18] found that the effect of increasing the polydispersivity of a distribution of hard spheres increased the effective transverse shear modulus G_e relative to monodispersions in most cases. However, they noted that in certain instances when the difference in phase moduli G_1 and G_2 was small, the polydispersivity may lead to a decrease in the effective property G_e. This difference between two and three dimensions is attributed to the different behavior of η_2 for cylinders relative to spheres noted in the previous section.

ACKNOWLEDGMENTS

The authors gratefully acknowledge the partial support of the Office of Basic Energy Sciences, U.S. Department of Energy, under Grant No. DE-FG05-86ER 13482 and of the Mars Mission Research Center (NASA Grant No. NAGW-1331), which is a cooperative effort of North Carolina State University and North Carolina A&T State University.

[1] S. Torquato, Rev. Chem. Eng. **4**, 151 (1987).
[2] S. Torquato, Appl. Mech. Rev. **44**, 37 (1991).
[3] R. Hill, J. Mech. Phys. Solids **12**, 199 (1964).
[4] Z. Hashin, J. Mech. Phys. Solids **13**, 119 (1965).
[5] Z. Hashin, in *Mechanics of Composite Materials*, edited by F. W. Wendt, H. Liebowitz, and N. Perrone (Pergamon), New York, 1970, p. 201.
[6] N. Silnutzer, Ph. D. thesis, University of Pennsylvania, Philadelphia, PA (1972).
[7] G. W. Milton, J. Mech. Phys. Solids **30**, 177 (1982).
[8] G. W. Milton, J. Appl. Phys. **52**, 5294 (1981).
[9] S. Torquato and J. D. Beasley, Int. J. Eng. Sci. **24**, 415 (1986).
[10] S. Torquato and J. D. Beasley, Int. J. Eng. Sci. **24**, 435 (1986).
[11] C. G. Joslin and G. Stell, J. Appl. Phys. **60**, 1607 (1986).
[12] C. G. Joslin and G. Stell, J. Appl. Phys. **60**, 1610 (1986).
[13] S. Torquato and F. Lado, Proc. R. Soc. London A **417**, 59 (1988).
[14] S. Torquato and F. Lado, J. Appl. Mech. (to be published).
[15] S. Torquato and G. Stell, J. Chem. Phys. **77**, 2071 (1982).
[16] S. Torquato and G. Stell, J. Chem. Phys. **82**, 980 (1985).
[17] P. A. Smith and S. Torquato, J. Appl. Phys. **65**, 893 (1989).
[18] J. F. Thovert, I. C. Kim, S. Torquato, and A. Acrivos, J. Appl. Phys. **67**, 6088 (1990).
[19] B. Lu and S. Torquato, Phys. Rev. A **43** (1991); (in press).
[20] S. Torquato, J. Stat. Phys. **45**, 843 (1986).
[21] C. A. Miller and S. Torquato, J. Appl. Phys. **68**, 5486 (1991).
[22] F. H. Stillinger, E. A. DiMarzio, and R. L. Kornegay, J. Chem. Phys. **40**, 1564 (1964).
[23] M. J. Beran and N. Silnutzer, J. Compos. Mater. **5**, 246 (1971).
[24] M. N. Miller, J. Math. Phys. **10**, 1988 (1969).
[25] S. Torquato and F. Lado, Phys. Rev. B **33**, 6428 (1986).
[26] S. Torquato, J. Appl. Phys. **58**, 3790 (1985).
[27] I. C. Kim and S. Torquato, J. Appl. Phys. **68**, 3892 (1990).